Can Disorder Enhance Incoherent Exciton Diffusion?

ARTICLE *in* THE JOURNAL OF PHYSICAL CHEMISTRY B · FEBRUARY 2015

Impact Factor: 3.3 · DOI: 10.1021/acs.jpcb.5b01886 · Source: arXiv

3 AUTHORS, INCLUDING:

Elizabeth M Y Lee

Massachusetts Institute of Technology

6 PUBLICATIONS **25** CITATIONS

SEE PROFILE

William A Tisdale

Massachusetts Institute of Technology

21 PUBLICATIONS **686** CITATIONS

SEE PROFILE

THE JOURNAL OF PHYSICAL CHEMISTRY B

Article

pubs.acs.org/JPCB

Can Disorder Enhance Incoherent Exciton Diffusion?

Elizabeth M. Y. Lee,[†] William A. Tisdale,[†] and Adam P. Willard*[,‡]

[†]Department of Chemical Engineering, Massachusetts Institute of Technology, Cambridge, Massachusetts 02139, United States

[‡]Department of Chemistry, Massachusetts Institute of Technology, Cambridge, Massachusetts 02139, United States

ABSTRACT: Recent experiments aimed at probing the dynamics of excitons have revealed that semiconducting films composed of disordered molecular subunits, unlike expectations for their perfectly ordered counterparts, can exhibit a time-dependent diffusivity in which the effective early time diffusion constant is larger than that of the steady state. This observation has led to speculation about what role, if any, microscopic disorder may play in enhancing exciton transport properties. In this article, we present the results of a model study aimed at addressing this point. Specifically, we introduce a general model, based upon Förster theory, for incoherent exciton diffusion in a material composed of independent molecular subunits with static energetic disorder. Energetic disorder leads to heterogeneity in molecule-to-molecule transition rates, which we demonstrate has two important consequences related to exciton transport. First, the distribution of local site-specific hopping rates is broadened in a manner that results in a decrease in average exciton diffusivity relative to that in a perfectly ordered film. Second, since excitons prefer to make transitions that are downhill in energy, the steady state distribution of exciton energies is biased toward low-energy molecular subunits, those that exhibit reduced diffusivity relative to a perfectly ordered film. These effects combine to reduce the net diffusivity in a manner that is time dependent and grows more pronounced as disorder is increased. Notably, however, we demonstrate that the presence of energetic disorder can give rise to a population of molecular subunits with exciton transfer rates exceeding those of subunits in an energetically uniform material. Such enhancements may play an important role in processes that are sensitive to molecular-scale fluctuations in exciton density field.

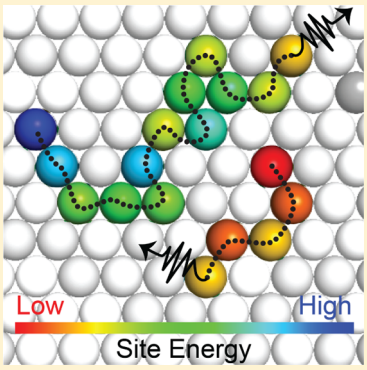

1. INTRODUCTION

Excitons are Coulombically bound electron−hole pairs that mediate the transport of energy in many molecular-scale systems. The dynamics of excitons are fundamental to processes such as photocurrent generation in solar cells,[1−6] photoluminescence in light emitting diodes (LEDs),[7−9] and photosynthetic light harvesting.[10−13] As with many electronic structure properties, the dynamics of excitons can be quite sensitive to the details of nuclear configuration. For materials that are amorphous or contain defects, the presence of molecular disorder is generally thought to hinder exciton transport properties,[14−17] for instance by reducing diffusivity;[15,17] however, it has been speculated that in certain cases disorder might serve to enhance exciton transport.[18,19]

The dynamics of excitons are diverse and highly system dependent. It is therefore useful to begin by establishing a language around which to frame our discussion. The general behavior of excitons, and how they migrate within systems composed of individual molecules, depend on the relative strength of intermolecular electronic coupling. Along these lines, we categorize exciton dynamics as being either *coherent* or *incoherent*, when the electronic coupling between neighboring molecular subunits is strong or weak, respectively.[13,20] In the coherent regime, excitons tend to delocalize across many individual molecular subunits, and their transport involves the collective interplay of nuclear and electronic degrees of freedom. In the incoherent regime, excitons tend to be localized on individual molecular subunits and migrate through a series of discrete molecule-to-molecule transitions. In practice, however, the facile characterization of exciton transport as being either coherent or incoherent can be misleading.

As early as the 1970s, pioneering work in the study of exciton dynamics[20−24] revealed that even in well-ordered systems, such as molecular crystals, careful consideration must be given to system properties that indirectly modulate intermolecular electronic coupling. Fluctuations in intermolecular spacing, such as those induced by phonon modes, or the presence of impurities, are some of the many effects that can serve to blur the boundary between coherent and incoherent exciton transport. These deliberations need to be taken in complicated systems such as biological assemblies, where the first spectroscopic evidence of quantum coherence in the photosynthetic light-harvesting system[10] inspired a flurry of experimental[25−29] and theoretical[12,17,18,30−37] studies. The result of this widespread scientific effort have been to establish that the highly efficient nanoscale transport of energy in biological systems arises due to an interplay between a coherent wave-like and an incoherent hopping dynamics. In photosynthetic systems, the synergy between local excitonic coherence and thermal environmental fluctuations results in higher energy transfer efficiencies than those that would be expected of purely coherent or purely incoherent transfer.[38]

Received: February 25, 2015
Revised: June 23, 2015

DOI: 10.1021/acs.jpcb.5b01886
J. Phys. Chem. B XXXX, XXX, XXX−XXX

In realistic physical systems, observed exciton transport reflects a complex interplay of coherent and incoherent-like dynamics, together with concomitant influences from an array of various sources of static and dynamic disorder.[13] The relative manifestation of these two regimes, in conjunction with the nature of static and dynamic disorder, is complicated and highly system dependent. For instance, sources of disorder vary widely in character, due to size polydispersity in colloidal quantum dots,[39] thermally induced fluctuations in the torsional angles[40] or relative molecular arrangements[41] in conjugated polymers, and dynamics of the protein conformation in light harvesting complexes.[42] Thus, deconvolving the complicated interaction of physical effects is intractable for all but the most simple systems.

A popular theoretical approach has been to begin from a simple reference system and include disorder in a tunable or systematic fashion. This approach has led to significant advances in our understanding of exciton dynamics in the coherent regime where the effects of disorder have been well studied in the context of general theoretical models. In most cases, static disorder has been shown to arrest diffusion via the phenomenon known as Anderson localization.[43] Nevertheless, the effect can be removed by the presence of dynamic disorder, for example, in the form of a system-bath coupling.[44] Our ability to analyze and interpret experimental data related to coherent exciton dynamics owes largely to the numerous studies[17,18,30−36] aimed at systematically exploring idealized systems with well-controlled disorder. Yet a more complete picture would also require accounting for the effects of disorder on the incoherent aspect of exciton dynamics, whose role can be significant.[45−50]

In this manuscript, we describe a study aimed at understanding the role of disorder on exciton dynamics in the incoherent regime. In our approach, we investigate the effect of a tunable source of disorder on an otherwise idealized model for exciton transport. Specifically, we consider the effect of static disorder in the excitation energy of molecular subunits on a purely incoherent model for exciton dynamics. The results offer insight into what contribution static, or slowly evolving, spatial disorder might play in the overall dynamics of excitons in more complicated systems. Our model is a two-dimensional weakly coupled array of chromophores. It bears resemblance to real physical systems such as colloidal quantum dots arrays,[3,49,51,52] certain organic semiconductor films,[40,45−48,50,53−55] as well as some molecular aggregates,[56,57] where at ambient conditions the coupling between the excitonic system and the environment is much stronger than the electronic coupling.

We determine that although site energetic disorder leads to a reduction in the average steady state diffusivity of excitons, microscopic heterogeneity gives rise to regions of the material for which exciton mobility is enhanced relative to that in the absence of disorder. We go on to show that the heterogeneity in microscopic transport properties is correlated with local excitation energy, and that this heterogeneity is responsible for the time-dependent diffusivity that has been observed by transient photoluminescene spectroscopy[46,58−61] as well as by more recently developed time-resolved optical microscopy.[60,62] In the next section, we describe our model for disordered incoherent exciton dynamics.

2. MODEL

We employ a simple and general model of a semiconductor film composed of a collection of disordered molecular subunits. Förster theory (perturbation method in the limit of strong system-bath coupling) provides the theoretical basis for our treatment of incoherent exciton dynamics.[63] In our model, excitons diffuse by performing a series of discrete hops between intermolecular subunits. Hopping rates are governed by the Förster rate equation,

$$k_{DA}(d, \varepsilon_D, \varepsilon_A) = \frac{1}{\tau}\left(\frac{R_0(\varepsilon_D, \varepsilon_A)}{d}\right)^6 \quad (1)$$

where d is the hopping distance, ε_D and ε_A are the absorption (excitation) energies of the donor and acceptor sites, respectively, τ is the experimentally determined exciton lifetime, and R_0 is the Förster radius. The dependence of exciton hopping rate on the excitation energies of molecular subunits is contained within the expression of the Förster radius,

$$R_0(\varepsilon_D, \varepsilon_A) = \left[\frac{9}{8\pi}\frac{c^4\hbar^4}{n^4}\eta\kappa^2\int\frac{\sigma(\varepsilon;\varepsilon_A)f(\varepsilon;\varepsilon_D)}{\varepsilon^4}\,d\varepsilon\right]^{1/6} \quad (2)$$

where n is the refractive index, c is the speed of light, $\hbar$ is the reduced Planck constant, η is the photoluminescence quantum yield, and κ is the transition dipole orientation factor. The term in the integral contains the overlap between the normalized emission spectrum, $f(\varepsilon;\varepsilon_D)$, of the donor molecule with site energy, ε_D, and the absorption spectrum, $\sigma(\varepsilon;\varepsilon_A)$, of the acceptor molecule with site energy ε_A. The Förster rate expression used here represents the classical limit (i.e., high temperature with a slowly relaxing bath) of an analogous but more general from of Fermi's golden rule.[64−66]

The line shapes of $\sigma(\varepsilon;\varepsilon_A)$ and $f(\varepsilon;\varepsilon_D)$ are taken to be Gaussian with a mean of ε_A and $\varepsilon_D - \Delta_{ss}$, respectively, and each with a standard deviation equal to the homogeneous line width σ_h. For a given molecular subunit, the difference in energy between the absorption and emission peaks is given by the Stokes shift, Δ_{ss}, which reflects the rapid (on the time scales of intermolecular excitonic transitions) electronic and nuclear relaxation that follows the excitation. Simulations are carried out in the dilute limit of exciton density. Statistics were averaged over 200 independent realizations of the molecular film (static disorder), and for each realization, approximately 700 000 single-exciton kinetic Monte Carlo trajectories. The standard deviation of the mean squared displacement at $t = \tau$ is less than 1% of the mean value.

We incorporate disorder into our model by varying the site energy (i.e., ε_A and ε_D in eqs 1 and 2) of individual molecular subunits. For this study, the model system consists of a two-dimensional array of 2500 hexagonally closed packed molecular subunits with absorption peak energies drawn randomly from a Gaussian distribution with mean $\bar{\varepsilon}$ and standard deviation σ_{ih}, corresponding to the inhomogeneous line width. Each molecular subunit is assigned a fixed transition dipole vector (used to generate κ in eq 2) oriented randomly on the surface of a unit sphere. The results displayed here utilize parameters and a system geometry that were selected to correspond to the thin film of CdSe/ZnCdS core−shell quantum dots (the subject of recent experiments[60]), such that the average Förster radius is $\langle R_0\rangle = 1.2d_0$. Nonetheless, we expect the qualitative features of our model to apply generally across systems

DOI: 10.1021/acs.jpcb.5b01886
J. Phys. Chem. B XXXX, XXX, XXX−XXX

exhibiting incoherent exciton transport with the Förster raidus that is on the order of, or slightly larger than, the interparticle spacing. The model system is described in greater detail in ref 60.

3. LOCAL EXCITON HOPPING RATE DEPENDS PRIMARILY ON DONOR SITE ENERGY

To understand exciton transport from a microscopic perspective, we consider the phenomenological rate for exciton transfer from an individual electronically excited molecular subunit. For condensed phase systems that exhibit incoherent exciton transport, this rate is dominated almost entirely by the sum of nearest neighbor molecule-to-molecule transitions, which are uniform and constant in a perfectly ordered film but vary upon the introduction of disorder. In our model, such variations arise from the dependence of eqs 1 and 2 on energetic disorder, through the variables ε_D and ε_A, and on spatial disorder, through the variables d and κ. From the perspective of an electronically excited donor molecule, the local environment provides a sampling of the system heterogeneity. For multidimensional systems, the dependence of exciton transfer rate on the environmental variables such as ε_A, d, and κ is mitigated by the population of many nearest neighbors. We can therefore understand the qualitative effect of site energetic disorder on exciton transport primarily in terms of the donor site energy by considering the average molecule-to-molecule transfer rate from a molecular subunit with site energy ε_D to a nearest neighbor site, given by

$$\bar{k}(\varepsilon_D) = \int_{-\infty}^{\infty} d\varepsilon_A k_{DA}(d_0, \varepsilon_D, \varepsilon_A) P(\varepsilon_A) \tag{3}$$

where d_0 is the nearest neighbor distance and $P(\varepsilon_A)$ is the distribution of site energies in the system,

$$P(\varepsilon_A) = \frac{1}{\sqrt{2\pi\sigma_{ih}^2}} \exp\left(-\frac{(\varepsilon_A - \bar{\varepsilon})^2}{2\sigma_{ih}^2}\right) \tag{4}$$

which is in this case Gaussian with mean $\bar{\varepsilon}$ and variance σ_{ih}. It turns out that even in two dimensions, the physics contained within eq 3 are sufficient to understand the general qualitative effects of energetic disorder on exciton transport.

For systems with symmetric and singly peaked energetic polydispersity, as is the case for this study, the expression in eq 3 can be simplified in the context of a mean field approximation to take the form $\bar{k}_{MF}(\varepsilon_D) = k_{DA}(d_0, \varepsilon_D, \bar{\varepsilon})$. Figure 1a contains a plot of $\bar{k}_{MF}(\varepsilon_D)$, where it is shown that the mean exciton hopping rate is a nonmonotonic function of donor site energy. The maximum transition rate is achieved when the donor site energy is above the average, specifically when $\varepsilon_D = \bar{\varepsilon} + \Delta_{ss}$,[67] where the magnitude of the donor−acceptor spectral overlap integral in eq 2 is optimized (see Figure 1b).

The nonmonotonic nature of $\bar{k}_{MF}(\varepsilon_D)$ shown in Figure 1a is a general feature that arises when the distribution of site energies is singly peaked. For example, we performed numerical simulations using non-Gaussian distributed static disorder (Cauchy and skewed gamma distributions, specifically) and obtained qualitatively similar results. Moreover, this non-monotonic hopping rate is due to the quantum mechanical resonance condition between the donor and the acceptor energy states. The classical analog to $\bar{k}_{MF}(\varepsilon_D)$ is a hopping rate that is a monotonic function of ε_D, in which more downhill energy transition corresponds to a larger rate. Although the two regimes (i.e., quantum and classical) predict similar behavior

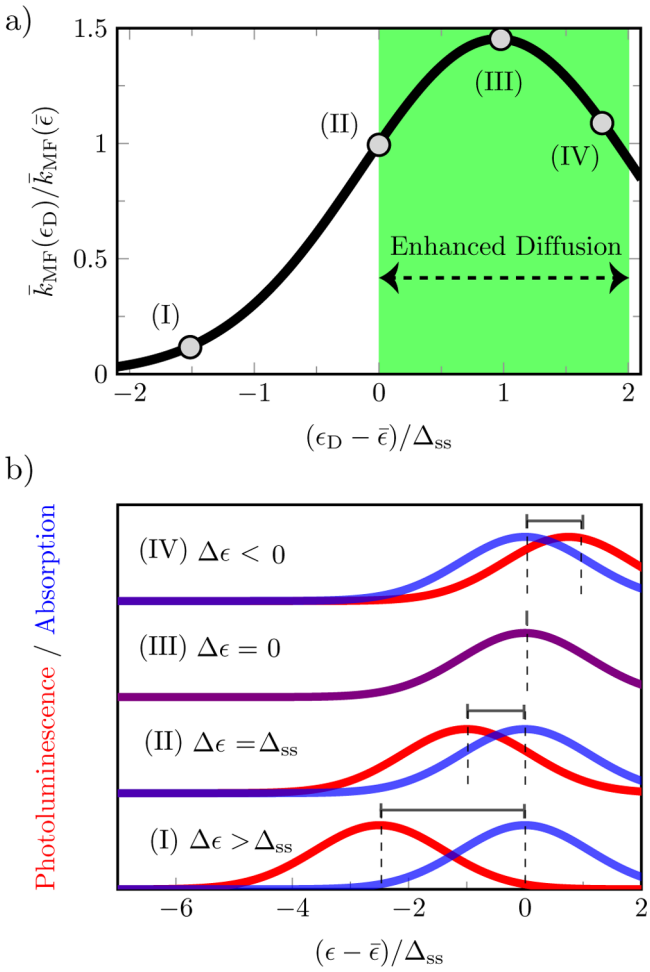

Figure 1. (a) The average pairwise energy transfer rates, $\bar{k}_{MF}(\varepsilon_D)$ between a donor molecule with site energy ε_D and an acceptor molecule with average site energy $\bar{\varepsilon}$. (b) The spectral overlap of the donor (red) and the acceptor (blue) subunits for selected values, numbered (I) through (IV), of $\bar{k}_{MF}(\varepsilon_D)$ as shown in panel a. The difference between the acceptor site energy (same as its absorption energy) and the donor emission energy (site energy offset by the Stokes shift, i.e., $\varepsilon_D - \Delta_{ss}$) is given by $\Delta\varepsilon = \bar{\varepsilon} - \varepsilon_D + \Delta_{ss}$. Subunits with site energies between $\bar{\varepsilon}$ and $\bar{\varepsilon} + 2\Delta_{ss}$, indicated by the shaded green region, exhibit exciton transfer rates that are enhanced relative to a perfectly uniform film. Hopping rates are calculated using eq 3 with a set of parameters ($\sigma_{ih} = 0.8\sigma_h$, $\sigma_h = 42$ meV, $\Delta_{ss} = 38$ meV, $n = 1.7$, $\eta = 1$, $d_0 = 8$ nm, $\kappa^2 = \langle\kappa^2\rangle = 2/3$, and $\tau = 10$ ns) that yields an average Förster radius of $\langle R_0\rangle = 1.2d_0$.

when state-to-state energy differences are small, they have been shown to result in nontrivial differences especially for systems prepared out of equilibrium.[46]

The exciton hopping rate illustrated in Figure 1a is a microscopic, single-molecule property. At the same time, the observed exciton transport properties of a material emerge through contributions of macroscopic ensemble of such molecules and thus depend on the statistics of microscopic disorder. In the next section, we evaluate the system-wide average hopping rate and discuss how it depends on the details of static disorder.

DOI: 10.1021/acs.jpcb.5b01886
J. Phys. Chem. B XXXX, XXX, XXX−XXX

4. THE EFFECT OF DISORDER ON THE MATERIAL-WIDE AVERAGE EXCITON HOPPING RATE

For the model in which the single-molecule absorption and its emission are governed by Gaussian statistics, we can analytically compare the average exciton hopping rate of films with and without energetic disorder to evaluate the net effect of site energetic disorder on the material-wide exciton hopping rates. From eqs 2 and 3, we see that in the absence of energetic disorder (i.e., $P(\varepsilon_A) = \delta(\varepsilon_A - \overline{\varepsilon})$), the nearest-neighbor exciton transfer rate is constant and is equal to

$$k_{DA}(d_0, \overline{\varepsilon}, \overline{\varepsilon}) = \frac{1}{\tau}\left(\frac{R_0(\overline{\varepsilon}, \overline{\varepsilon})}{d_0}\right)^6 = C\int_{-\infty}^{\infty} d\varepsilon \frac{1}{\varepsilon^4} \exp\left(-\frac{(\overline{\varepsilon} - \varepsilon)^2}{2\sigma_h^2}\right)\frac{1}{\sqrt{2\pi\sigma_h^2}} \times \exp\left(-\frac{(\overline{\varepsilon} - \Delta_{ss} - \varepsilon)^2}{2\sigma_h^2}\right) \tag{5}$$

$$= \frac{C}{\sqrt{2}}\frac{1}{\left(\overline{\varepsilon} - \frac{\Delta_{ss}}{2}\right)^4} \exp\left(-\frac{\Delta_{ss}^2}{4\sigma_h^2}\right) \tag{6}$$

where C is a collection of physical constants,

$$C \equiv \frac{9}{8\pi}\frac{c^4\hbar^4}{n^4}\eta\sigma(\overline{\varepsilon})\langle\kappa^2\rangle\frac{1}{\tau d_0^6} \tag{7}$$

which includes the absorption cross section σ at $\overline{\varepsilon}$, $\sigma(\overline{\varepsilon})$, and the average dipole orientation factor, $\langle\kappa^2\rangle = 2/3$. The expression in eq 6 reflects the assumption that the ε^4 term does not vary significantly over the Gaussian term with respect to ε in eq 5,[47] which is valid in cases where the line width is smaller than the band gap.

For a film *with* energetic disorder, the nearest-neighbor exciton transfer rate depends on exciton energy, as illustrated in Figure 1a. Notably, the molecular subunits with site energies between $\overline{\varepsilon}$ and $\overline{\varepsilon} + 2\Delta_{ss}$ exhibit exciton transfer rates that are enhanced relative to a perfectly ordered film. However, a consequence of the nonmonotonic turnover in exciton transfer rates for $\varepsilon_D > \overline{\varepsilon} + \Delta_{ss}$ is that the system-wide average exciton transfer rate is expected to be reduced relative to that of an energetically ordered system. More formally, the film-wide average exciton transfer rate is given by

$$\langle k\rangle = \int_{-\infty}^{\infty} d\varepsilon_D \overline{k}(\varepsilon_D)P(\varepsilon_D) = \int_{-\infty}^{\infty}\int_{-\infty}^{\infty} d\varepsilon_D d\varepsilon_A k_{DA}(d_0, \varepsilon_D, \varepsilon_A)P(\varepsilon_A)P(\varepsilon_D) \tag{8}$$

Since $P(\varepsilon_D)$ and $P(\varepsilon_A)$ are Gaussian density of states centered at $\overline{\varepsilon}$ for both donors and acceptors as defined in eq 4, eq 8 can be rewritten as

$$\langle k\rangle = \frac{C}{(2\pi)^{3/2}\sigma_{ih}^2\sigma_h}\int_{-\infty}^{\infty}\int_{-\infty}^{\infty}\int_{-\infty}^{\infty}\frac{d\varepsilon_A d\varepsilon_D d\varepsilon}{\varepsilon^4}\exp\left(-\frac{(\varepsilon_A - \overline{\varepsilon})^2}{2\sigma_{ih}^2}\right) \times \exp\left(-\frac{(\varepsilon_A - \varepsilon)^2}{2\sigma_h^2}\right)\exp\left(-\frac{(\varepsilon_D - \overline{\varepsilon})^2}{2\sigma_{ih}^2}\right)\exp\left(-\frac{(\varepsilon_D - \Delta_{ss} - \varepsilon)^2}{2\sigma_h^2}\right) \tag{9}$$

To evaluate eq 9, we first integrate with respect to ε_A and ε_D and then ε because the terms involving ε_A and ε_D are independent from one another while ε is dependent on other two variables. This leads to

$$\langle k\rangle = \frac{C}{\sqrt{2\pi\sigma_h^2}}\frac{1}{\beta^2 + 1}\int_{-\infty}^{\infty}\frac{d\varepsilon}{\varepsilon^4} \times \exp\left[-\frac{\left(\varepsilon - \left(\overline{\varepsilon} - \frac{\Delta_{ss}}{2}\right)\right)^2}{(\beta^2 + 1)\sigma_h^2}\right]\exp\left[-\frac{\Delta_{ss}^2}{4(\beta^2 + 1)\sigma_h^2}\right] \tag{10}$$

where $\beta \equiv \sigma_{ih}/\sigma_h$ is the ratio of static disorder to the dynamic disorder. Again, assuming that the ε^4 term does not vary significantly over the Gaussian term with respect to ε in eq 10, we can simplify the above equation as

$$\langle k\rangle = \frac{C}{\sqrt{2}}\frac{1}{\sqrt{\beta^2 + 1}}\frac{1}{\left(\overline{\varepsilon} - \frac{\Delta_{ss}}{2}\right)^4}\exp\left[-\frac{\Delta_{ss}^2}{4(\beta^2 + 1)\sigma_h^2}\right] \tag{11}$$

which can be rewritten in terms of the original variables as

$$\langle k\rangle = \frac{C}{\sqrt{2}}\frac{\sigma_h}{\sqrt{\sigma_{ih}^2 + \sigma_h^2}}\frac{1}{\left(\overline{\varepsilon} - \frac{\Delta_{ss}}{2}\right)^4}\exp\left[-\frac{\Delta_{ss}^2}{4(\sigma_{ih}^2 + \sigma_h^2)}\right] \tag{12}$$

By comparing eqs 6 and 12, we find that the average exciton transfer rate is decreased by disorder (i.e., $\langle k\rangle < k_{DA}(d_0, \overline{\varepsilon}, \overline{\varepsilon})$) if

$$\left(\frac{\Delta_{ss}}{\sigma_h}\right)^2 < \frac{2(1 + \beta^2)}{\beta^2}\ln(1 + \beta^2) \tag{13}$$

The right-hand side of eq 13 is a monotonically increasing function of β^2, and also is greater than or equal to 2, with the equality occurring when $\beta = 0$. Therefore, the necessary condition for which the average exciton hopping rate for an energetically disordered film (i.e., some nonzero value of β) can be enhanced relative to that of an ordered film (e.g., $\langle k\rangle > k_{DA}(d_0, \overline{\varepsilon}, \overline{\varepsilon})$ is

$$\left(\frac{\Delta_{ss}}{\sigma_h}\right)^2 > 2 \tag{14}$$

The value on the right-hand side of eq 13 grows with β and is thus larger than 2 for typical systems (e.g., 2.5 for the system considered here in which $\beta = 0.8$).

Equations 13 and 14 tell us that energetic disorder *only* serves to enhance the film-wide average exciton transfer rate when the ordered system has poor donor−acceptor spectral overlap, in which case disorder serves to facilitate energetic resonance between some nearest neighbor pairs. For example, certain materials such as colloidal quantum dots[68,69] and organic fluorophores[70] can be engineered to exhibit a large Stokes shift to reduce self-energy transfer or reabsorption for applications in luminescent solar concentrators or biological labeling. A schematic example of a system that obeys the inequality of eq 14 (thus exhibiting disorder-enhanced exciton diffusivity) is shown in Figure 2. When static disorder is small, such as in Figure 2a, the donor−acceptor spectral overlap that

DOI: 10.1021/acs.jpcb.5b01886
J. Phys. Chem. B XXXX, XXX, XXX−XXX

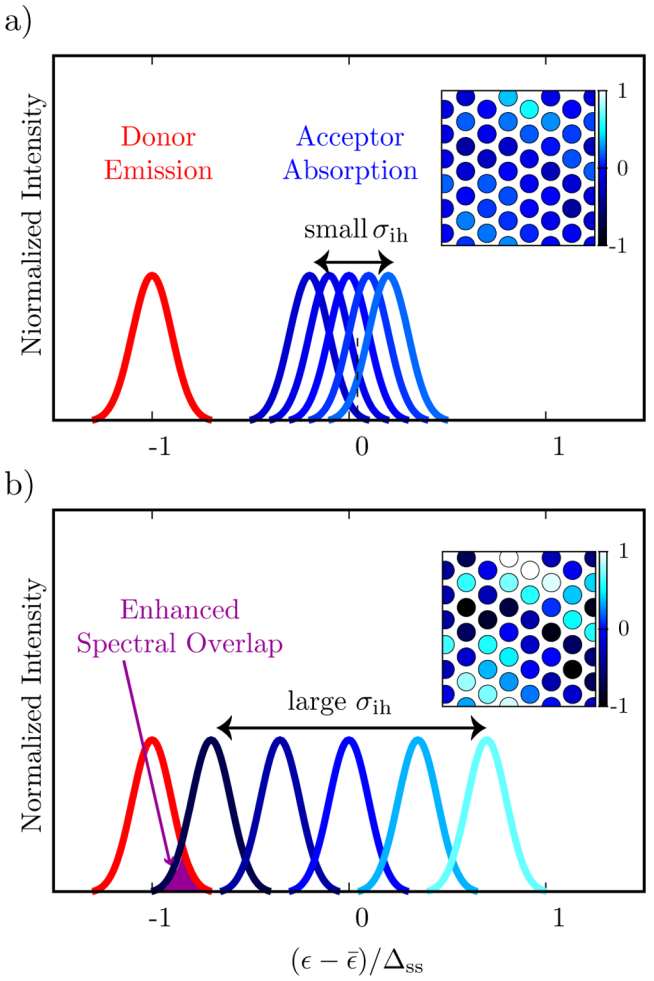

Figure 2. A hypothetical system for which global exciton diffusivity is enhanced by disorder (i.e., where $\Delta_{ss}/\sigma_h > 2$ as in eq 14). We illustrate the enhancement by considering the normalized emission intensity of a single donor molecule (plotted in red) alongside normalized absorption intensities of neighboring acceptor molecules (plotted in blue). In each panel, the values of the Stokes shift, Δ_{ss}, and homogeneous line width, σ_h, are identical. In panel a, the inhomogeneous line width, σ_{ih}, is small relative to σ_h, while in panel b σ_{ih} is large relative to σ_h. The difference in σ_{ih} is illustrated in the panel inset, which contains a schematic depiction of the film with sites colored corresponding to their relative energies (individual absorption peaks according to the same color scale). In panel a, there is negligible donor−acceptor overlap, while in panel b energetic disorder enables enhanced spectral overlap (indicated with violet shading), thereby facilitating site-to-site exciton hopping.

enables site-to-site energy transfer is vanishingly small. Here, as illustrated by comparing Figures 2a and 2b, increasing site-energetic disorder facilitates spectral overlap between some neighboring donor−acceptor pairs, thereby leading to an enhancement in the overall average hopping rate of the system.

A similar type of analysis can be carried out with respect to spatial disorder in which the molecule-to-molecule transition rates are modulated through the d-dependence (or κ-dependence) of eq 1. The results are analogous to those described above: the presence of spatial disorder typically leads to a reduction in the film-wide average exciton transfer rate.

The observed rate of exciton transfer is only equal to the material-wide average when excitons are uniformly distributed across the ensemble of molecular subunits. Energetic disorder, however, has another important effect on exciton transport in that it facilitates the time-varying dissipation of excitation energy, thereby biasing excitons toward lower-energy molecular subunits (see Figure 1a). In the next section, we employ Monte Carlo simulations to explore time-dependent effect of energetic relaxation on observed exciton diffusivity.

5. TRANSIENT ENERGETIC RELAXATION LEADS TO TIME DEPENDENT EXCITON DIFFUSIVITY

Each energy transfer event is associated with small energetic losses. In our model, the dissipative mechanism appears in the form of the Stokes shift, Δ_{ss}, designed to mimic the rapid internal electronic and nuclear relaxation that follows molecular excitation. Because of the Stokes shift, the most probable transitions—those that maximize overlap between donor emission and acceptor absorption line shapes—are energy transfer events from donor to acceptor molecules, with the acceptor molecules having excitation energies that are Δ_{ss} lower than the donor molecules. Therefore, the initial diffusion of randomly populated excitons is accompanied by a decrease in average exciton energy.

Using a standard kinetic Monte Carlo algorithm to study the dynamics of excitons, we analyze the trajectories of individual noninteracting excitons with a particular focus on the relationship between exciton energy and diffusivity. Figure 3a compares the time-dependent average displacement of a uniform distribution of excitons in an energetically disordered film to that in a film without energetic disorder. The average displacement is computed as $\langle |R| \rangle(t) \equiv \sqrt{\langle (\mathbf{r}(t) - \mathbf{r}(0))^2 \rangle}$, where $r(t)$ denotes the position of the exciton at time t (here, $t = 0$ is the time of excitation) and angle brackets represent an average over the ensemble of trajectories.

We observe that excitons within the disordered film (see the curve labeled as "disorder" in Figure 3a) exhibit reduced diffusivity when compared to a perfectly ordered film (see the curve labeled "uniform" in Figure 3a). In addition, we show the average displacement for two subpopulations of excitons: one initialized on high energy molecular subunits (those with excitation energies $\epsilon_i = \bar{\epsilon} + \Delta_{ss}$) and the other initilized on low energy molecular subunits (those with excitation energies $\epsilon_i = \bar{\epsilon} - 0.8\Delta_{ss}$). We observe that the initial behavior of either subpopulation is consistent with the results plotted in Figure 1a, namely, that excitons with low initial energies diffuse more slowly than the ensemble average, while excitons with high initial energies diffuse more rapidly than the ensemble average. The high energy excitons even manifest a short time enhancement in diffusivity relative to that of an energetically uniform film. The enhancement in diffusion for high-energy excitons is short-lived because this population of excitons rapidly thermalizes, preferring to occupy lower energy molecular subunits whose effective hopping rates no longer reflect their initial enhancement (see Figure 1a). Consequently, over time scales that permit multiple site-to-site transitions, the average distance traveled by excitons, regardless of their initial energy, becomes less than the average distance traveled by excitons in the absence of energetic disorder.

Evidence for the rapid dissipation of energy for the *diffusion-enhanced* excitons can be seen by analyzing the transient energetics of simulated exciton trajectories (represented by line color in Figure 3a). In particular, the line color in Figure 3 corresponds to the mean site energy, averaged over a given population of excitons, at a specific time t. In contrast to the

DOI: 10.1021/acs.jpcb.5b01886
J. Phys. Chem. B XXXX, XXX, XXX−XXX

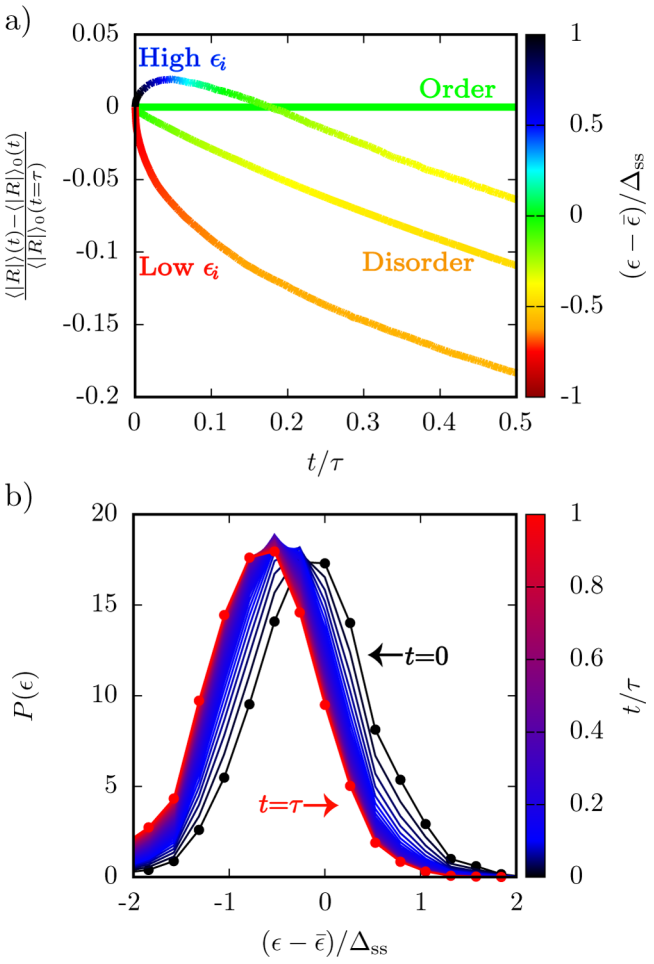

Figure 3. Exciton dynamics within energetically disordered molecular film. (a) The average diffusion length of excitons in a disordered film plotted relative to those in an energetically ordered film, the latter denote by $\langle |R| \rangle_0(t)$. The four curves correspond to the ordered film result, an average over excitons initialized uniformly across within a disordered film (the curve labeled *disorder*) and an average over the subpopulation of excitons initialized on either high energy (labeled high ε_i) or low energy (labeled low ε_i) sites. This quantity has been normalized by the diffusion length in the ordered film measured at the exciton's lifetime ($\langle |R| \rangle_0(t = \tau)$). The average site energy visited by the exciton is indicated by its correpsonding color. (Blue is high, and red is low energy.) (b) Time-evolution of the probability density distribution of excitons with energy ε. Time points are indicated by its corresponding color. (Black is the initial state, and red is the state in which most excitons have already decayed.)

rapid energetic decrease observed in the population of excitons with initially high energies, excitons with initially low energies exhibit an initial increase in energy, indicating that the lowest energy sites are not traps but are dynamically repopulated. The transient energetics can be better understood by considering the time-dependent distribution of exciton energies (see Figure 3b).

In Figure 3b, we plot $P(\varepsilon)$, the probability that an exciton resides on a molecular subunit with site energy, ε. The probability is resolved as a function of time, where at $t = 0$ excitons are uniformly distributed across the all molecular subunits. We observe a pronounced transient red-shift starting from an initially uniform distribution (black line in Figure 3b) to a final near steady state distribution (red lines in Figure 3b). This phenomenon is the result of individual excitons performing energy lowering molecule-to-molecule transitions. During the nonequilibrium relaxation, the population of excitons residing on molecular subunits with enhanced hopping rates (relative to systems without energetic disorder) decreases rapidly with time, which is accompanied by a corresponding increase in the population of excitons that reside on sites with reduced hopping rates (relative to a system without energetic disorder). The combined effect is a time-dependent lowering of net exciton diffusivity as more excitons occupy molecular subunits with low energy and reduced intermolecular transition rates.

The relationship between static energetic disorder and transient energetics has been previously explored in detail by Bässler[71] for free carriers. The phenomenon for excitons is experimentally measurable through the time-dependence of the fluorescence spectrum.[58,60] Similarly, the relationship between static energy disorder and exciton transport is experimentally accessible through the time- and position-dependence of the fluorescence spectrum[46,60,62] where the transient lowering of net exciton diffusivity manifests itself in the mean squared displacement (MSD), $\langle (\mathbf{r}(t) - \mathbf{r}(0))^2 \rangle$. In the absence of disorder (i.e., $\sigma_{ih} = 0$), exciton transport is diffusive (i.e., $\langle (\mathbf{r}(t) - \mathbf{r}(0))^2 \rangle \propto t$) at all times.[72] At the same time, static disorder gives rise to exciton transport that appears subdiffusive (i.e., $\langle (\mathbf{r}(t) - \mathbf{r}(0))^2 \rangle \propto t^{\alpha}$, where $\alpha < 1$). In fact, the connection to anomalous diffusion[47,57,60,73] is superficial, as the nonlinear behavior in Figure 4 is actually a nonequilibrium effect whose

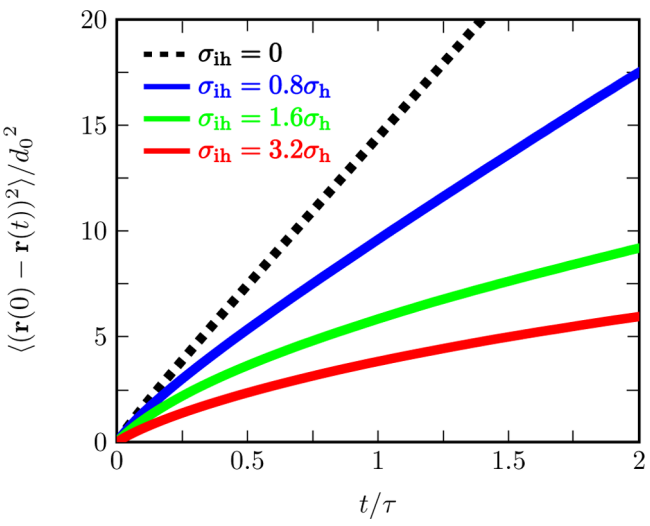

Figure 4. Mean square displacements (MSD), $\langle (\mathbf{r}(t) - \mathbf{r}(0))^2 \rangle$, of excitons in molecular films with various degrees of site energetic disorder. MSD is normalized by the square of the nearest neighbor distance, d_0, such that $\langle (\mathbf{r}(t) - \mathbf{r}(0))^2 \rangle / d_0^2$ is proportional to the square of the number of exciton hops. In the presence of static disorder, $\langle (\mathbf{r}(t) - \mathbf{r}(0))^2 \rangle$ is shorter than that of the uniform energy case, $\sigma_{ih} = 0$, at all times.

origin is tied to the time-dependent relaxation of the population of exciton energies (e.g., see Figure 3b). Nonlinearities in exciton diffusion have been observed experimentally via ultrafast spatially resolved spectroscopy but otherwise vanish over time scales of energetic exciton relaxation.[60] The net effect of disorder is to reduce the mean squared displacement of excitons in a manner that grows more pronounced as disorder is increased and as the time from initial excitation grows. This conclusion is invariant for other types of static disorder

DOI: 10.1021/acs.jpcb.5b01886
J. Phys. Chem. B XXXX, XXX, XXX−XXX

distribution that we have studied (e.g., Cauchy distribution and bimodal distribution with two symmetric Gaussian peaks) or by others.[57]

Additionally, the extent of initial deviations from the $\sigma_{ih} = 0$ case depends sensitively on the extent of static disorder, as does the steady state diffusion constant (i.e., the slope of MSD at long times).

6. CONCLUSIONS

In summary, using a simple Förster-type model of incoherent exciton dynamics in an energetically disordered array of molecular subunits, we have shown that site-energetic disorder leads to variations in transport properties of individual molecular subunits. The variations correlate with site energy, which can be understood in terms of spectral overlap integrals, and have the net effect of reducing the average molecule-to-molecule transition rate relative to that of a perfectly ordered material. Furthermore, in the presence of disorder, the steady state distribution of exciton energies is not identical to the distribution of site energies due to the dissipation of electronic energy that accompanies typical molecule-to-molecule transitions. Consequently, the steady state distribution of excitons is biased toward sites with lower than average excitation energies, and thus with exciton transfer rates that are reduced relative to that in an ordered material. Hence the observed exciton diffusivity is further lowered by transient exciton diffusion. The answer to the question posed in the title of this article is length and time scale dependent. For macroscopic systems, the answer is *no*: the average effect of disorder is to reduce overall exciton transport. However, at the nanoscale, the answer is *yes*: disorder can serve to enhance exciton mobility in certain microscopic regions. Considering such microscopic enhancements, along with their diminishing counterparts, will become increasingly important as devices continue to incorporate nanotechnological elements.

AUTHOR INFORMATION

Corresponding Author

*Phone: +1 (617) 253-1480; E-mail: awillard@mit.edu.

Notes

The authors declare no competing financial interest.

ACKNOWLEDGMENTS

E.M.Y.L thanks Chee Kong Lee and Liang Shi for helpful discussions. E.M.Y.L. gratefully acknowledges fellowship support from the National Science Foundation Graduate Research Fellowship Program under Grant 1122374.

REFERENCES

(1) Coakley, K. M.; McGehee, M. D. Conjugated Polymer Photovoltaic Cells. *Chem. Mater.* **2004**, *16*, 4533−4542.
(2) Mayer, A.; Scully, S.; Hardin, B.; Rowell, M.; Mcghee, M. Polymer-Based Solar Cells. *Mater. Today* **2007**, *10*, 28−33.
(3) Nozik, A. J. Multiple Exciton Generation in Semiconductor Quantum Dots. *Chem. Phys. Lett.* **2008**, *457*, 3−11.
(4) Servaites, J. D.; Ratner, M. A.; Marks, T. J. Organic Solar Cells: A New Look at Traditional Models. *Energy Environ. Sci.* **2011**, *4*, 4410−4422.
(5) Menke, S. M.; Luhman, W. A.; Holmes, R. J. Tailored Exciton Diffusion in Organic Photovoltaic Cells for Enhanced Power Conversion Efficiency. *Nat. Mater.* **2012**, *12*, 152−157.
(6) Graetzel, M.; Janssen, R. A. J.; Mitzi, D. B.; Sargent, E. H. Materials Interface Engineering for Solution-Processed Photovoltaics. *Nature* **2012**, *488*, 304−312.
(7) Baldo, M. A.; Thompson, M. E.; Forrest, S. R. High-Efficiency Fluorescent Organic Light-Emitting Devices Using a Phosphorescent Sensitizer. *Nature* **2000**, *403*, 750−753.
(8) Burin, A. L.; Ratner, M. A. Exciton Migration and Cathode Quenching in Organic Light Emitting Diodes. *J. Phys. Chem. A* **2000**, *104*, 4704−4710.
(9) Mashford, B. S.; Stevenson, M.; Popovic, Z.; Hamilton, C.; Zhou, Z.; Breen, C.; Steckel, J.; Bulovic, V.; Bawendi, M.; Coe-Sullivan, S.; et al. High-Efficiency Quantum-Dot Light-Emitting Devices with Enhanced Charge Injection. *Nat. Photonics* **2013**, *7*, 407−412.
(10) Engel, G. S.; Calhoun, T. R.; Read, E. L.; Ahn, T.-K.; Mancal, T.; Cheng, Y.-C.; Blankenship, R. E.; Fleming, G. R. Evidence for Wavelike Energy Transfer Through Quantum Coherence in Photosynthetic Systems. *Nature* **2007**, *446*, 782−786.
(11) Olaya-Castro, A.; Nazir, A.; Fleming, G. R. Quantum-coherent Energy Transfer: Implications for Biology and New Energy Technologies. *Philos. Trans. R. Soc. A* **2012**, *370*, 3613−3617.
(12) Kassal, I.; Yuen-Zhou, J.; Rahimi-Keshari, S. Does Coherence Enhance Transport in Photosynthesis? *J. Phys. Chem. Lett.* **2013**, *4*, 362−367.
(13) Chenu, A.; Scholes, G. D. Coherence in Energy Transfer and Photosynthesis. *Annu. Rev. Phys. Chem.* **2015**, *66*, 69−96.
(14) Bakalis, L. D.; Knoester, J. Pump-Probe Spectroscopy and the Exciton Delocalization Length in Molecular Aggregates. *J. Phys. Chem. B* **1999**, *103*, 6620−6628.
(15) Markov, D.; Tanase, C.; Blom, P.; Wildeman, J. Simultaneous Enhancement of Charge Transport and Exciton Diffusion in Poly(*p*-phenylene vinylene) Derivatives. *Phys. Rev. B* **2005**, *72*, 045217.
(16) Lunt, R. R.; Benziger, J. B.; Forrest, S. R. Relationship Between Crystalline Order and Exciton Diffusion Length in Molecular Organic Semiconductors. *Adv. Mater.* **2010**, *22*, 1233−1236.
(17) Moix, J. M.; Khasin, M.; Cao, J. Coherent Quantum Transport in Disordered Systems: I. The Influence of Dephasing on the Transport Properties and Absorption Spectra on One-dimensional Systems. *New J. Phys.* **2013**, *15*, 085010.
(18) Mohseni, M.; Rebentrost, P.; Lloyd, S.; Aspuru-Guzik, A. Environment-assisted Quantum Walks in Photosynthetic Energy Transfer. *J. Chem. Phys.* **2008**, *129*, 174106.
(19) Lee, C. K.; Moix, J.; Cao, J. Coherent Quantum Transport in Disordered Systems: A Unified Polaron Treatment of Hopping and Band-like Transport. *J. Chem. Phys.* **2015**, *142*, 164103.
(20) Silbey, R. *Electronic Energy Transfer in Molecular Crystals* **1976**, *27*, 203−223.
(21) Grover, M.; Silbey, R. Exciton Migration in Molecular Crystals. *J. Chem. Phys.* **1971**, *54*, 4843−4851.
(22) Haken, H.; Reineker, P. The Coupled Coherent and Incoherent Motion of Excitons and Its Influence on the Line Shape of Optical Absorption. *Z. Physik* **1972**, *249*, 253−268.
(23) Haken, H.; Strobl, G. An Exactly Solvable Model for Coherent and Incoherent Exciton Motion. *Z. Phys.* **1973**, *262*, 135−148.
(24) Kenkre, V. M.; Knox, R. S. Theory of Fast and Slow Excitation Transfer Rates. *Phys. Rev. Lett.* **1974**, *33*, 803−806.
(25) Liu, S. G.; Carlson, R. M. K.; Tucciarone, A. Coherence Dynamics in Photosynthesis: Protein Protection of Excitonic Coherence. *Science* **2007**, *316*, 1462−1465.
(26) Ahn, T. K.; Avenson, T. J.; Ballottari, M.; Cheng, Y.-C.; Niyogi, K. K.; Bassi, R.; Fleming, G. R. Architecture of a Charge-Transfer State Regulating Light Harvesting in a Plant Antenna Protein. *Science* **2008**, *320*, 794−797.
(27) Collini, E.; Scholes, G. Coherent Intrachain Energy Migration in a Conjugated Polymer at Room Temperature. *Science* **2009**, 369−373.
(28) Greyson, E. C.; Vura-Weis, J.; Michl, J.; Ratner, M. A. Maximizing Singlet Fission in Organic Dimers: Theoretical Investigation of Triplet Yield in the Regime of Localized Excitation and Fast Coherent Electron Transfer. *J. Phys. Chem. B* **2010**, *114*, 14168−14177.

DOI: 10.1021/acs.jpcb.5b01886
J. Phys. Chem. B XXXX, XXX, XXX−XXX

(29) Nelson, T.; Fernandez-Aberti, S.; Chernyak, V.; Roitberg, A. E.; Tretiak, S. Nonadiabatic Excited-state Molecular Dynamics Modeling of Photoinduced Dynamics in Conjugated Molecules. *J. Phys. Chem. B* **2011**, *115*, 5402−5414.
(30) Olaya-Castro, A.; Lee, C. F.; Olsen, F. F.; Johnson, N. F. Efficiency of Energy Transfer in a Light-Harvesting System under Quantum Coherence. *Phys. Rev. B* **2008**, *78*, 1−7.
(31) Plenio, M. B.; Huelga, S. F. Dephasing-Assisted Transport: Quantum Networks and Biomolecules. *New J. Phys.* **2008**, *10*, 113019.
(32) Cao, J.; Silbey, R. J. Optimization of Exciton Trapping in Energy Transfer Processes. *J. Phys. Chem. A* **2009**, *113*, 13825−13838.
(33) Ishizaki, A.; Fleming, G. R. Theoretical Examination of Quantum Coherence in a Photosynthetic System at Physiological Temperature. *Proc. Natl. Acad. Sci. U.S.A.* **2009**, *106*, 17255−17260.
(34) Ishizaki, A.; Fleming, G. R. On the Adequacy of the Redfield Equation and Related Approaches to the Study of Quantum Dynamics in Electronic Energy Transfer. *J. Chem. Phys.* **2009**, *130*, 234110.
(35) Ishizaki, A.; Fleming, G. R. Unified Treatment of Quantum Coherent and Incoherent Hopping Dynamics in Electronic Energy Transfer: Reduced Hierarchy Equation Approach. *J. Chem. Phys.* **2009**, *130*, 234111.
(36) Chen, X.; Silbey, R. J. Effect of Correlation of Local Fluctuations on Exciton Coherence. *J. Chem. Phys.* **2010**, *132*, 204503.
(37) Valleau, S.; Saikin, S. K.; Yung, M.-H.; Aspuru Guzik, A. Exciton Transport in Thin-film Cyanine Dye J-aggregates. *J. Chem. Phys.* **2012**, *137*, 034109.
(38) Ringsmuth, A. K.; Milburn, G. J.; Stace, T. M. Multiscale Photosynthetic and Biomimetic Excitation Energy Transfer. *Nat. Phys.* **2012**, *8*, 562−567.
(39) Cui, J.; Beyler, A. P.; Marshall, L. F.; Chen, O.; Harris, D. K.; Wanger, D. D.; Brokmann, X.; Bawendi, M. G. Direct Probe of Spectral Inhomogeneity Reveals Synthetic Tunability of Single-nanocrystal Spectral Linewidths. *Nat. Chem.* **2013**, *5*, 602−606.
(40) Barford, W.; Trembath, D. Exciton Localization in Polymers with Static Disorder. *Phys. Rev. B* **2009**, *80*, 165418.
(41) Jailaubekov, A. E.; Willard, A. P.; Tritsch, J. R.; Chan, W.-L.; Sai, N.; Gearba, R.; Kaake, L. G.; Williams, K. J.; Leung, K.; Rossky, P. J.; et al. Hot Charge-transfer Excitons Set the Time Limit for Charge Separation at Donor/Acceptor Interfaces in Organic Photovoltaics. *Nat. Mater.* **2012**, *12*, 66−73.
(42) Moix, J. M.; Zhao, Y.; Cao, J. Equilibrium-reduced Density Matrix Formulation: Influence of Noise, Disorder, and Temperature on Localization in Excitonic Systems. *Phys. Rev. B* **2012**, *85*, 1−14.
(43) Anderson, P. W. Absence of Diffusion in Certain Random Lattices. *Phys. Rev.* **1958**, *109*, 1492−1505.
(44) Evensky, D. A.; Scalettar, R. T.; Wolynes, G. Localization and Dephasing Effects in a Time-Dependent Anderson Hamiltonian. *J. Phys. Chem.* **1990**, *94*, 1149−1154.
(45) Burlakov, V.; Kawata, K.; Assender, H.; Briggs, G.; Ruseckas, A.; Samuel, I. Discrete Hopping Model of Exciton Transport in Disordered Media. *Phys. Rev. B* **2005**, *72*, 075206.
(46) Madigan, C.; Bulović, V. Modeling of Exciton Diffusion in Amorphous Organic Thin Films. *Phys. Rev. Lett.* **2006**, *96*, 046404.
(47) Ahn, T.-S.; Wright, N.; Bardeen, C. J. The Effects of Orientational and Energetic Disorder on Förster Energy Migration Along a One-dimensional Lattice. *Chem. Phys. Lett.* **2007**, *446*, 43−48.
(48) Singh, J.; Bittner, E. R.; Beljonne, D.; Scholes, G. D. Fluorescence Depolarization in Poly[2-methoxy-5-((2-ethylhexyl)-oxy)-1,4- phenylenevinylene]: Sites Versus Eigenstates Hopping. *J. Chem. Phys.* **2009**, *131*, 194905.
(49) Miyazaki, J.; Kinoshita, S. Site-selective Spectroscopic Study on the Dynamics of Exciton Hopping in an Array of Inhomogeneously Broadened Quantum Dots. *Phys. Rev. B* **2012**, *86*, 035303.
(50) Tapping, P. C.; Clafton, S. N.; Schwarz, K. N.; Kee, T. W.; Huang, D. M. Molecular-Level Details of Morphology-Dependent Exciton Migration in Poly(3-hexylthiophene) Nanostructures. *J. Phys. Chem. C* **2015**, *119*, 7047−7059.
(51) Alivisatos, A. P. Semiconductor Clusters, Nanocrystals, and Quantum Dots. *Science* **1996**, *271*, 933−937.
(52) Talapin, D. V.; Lee, J.-S.; Kovalenko, M. V.; Shevchenko, E. V. Prospects of Colloidal Nanocrystals for Electronic and Optoelectronic Applications. *Chem. Rev.* **2010**, *110*, 389−458.
(53) Pope, M.; Swenberg, C. E. *Electronic Processes in Organic Crystals and Polymers*, 2nd ed.; Oxford University Press: New York, 1999.
(54) Bardeen, C. J. Excitonic Processes in Molecular Crystalline Materials. *MRS Bull.* **2013**, *38*, 65−71.
(55) Wong, C. Y.; Cotts, B. L.; Wu, H.; Ginsberg, N. S. Exciton Dynamics Reveal Aggregates with Intermolecular Order at Hidden Interfaces in Solution-Cast Organic Semiconducting Films. *Nat. Commun.* **2015**, *6*, 5946.
(56) Fidder, H.; Knoester, J.; Wiersma, D. A. Optical Properties of Disordered Molecular Aggregates: A Numerical Study. *J. Chem. Phys.* **1991**, *95*, 7880−7890.
(57) Vlaming, S. M.; Malyshev, V. A.; Eisfeld, A.; Knoester, J. Subdiffusive Exciton Motion in Systems with Heavy-Tailed Disorder. *J. Chem. Phys.* **2013**, *138*, 214316.
(58) Crooker, S. A.; Hollingsworth, J. A.; Tretiak, S.; Klimov, V. I. Spectrally Resolved Dynamics of Energy Transfer in Quantum-Dot Assemblies: Towards Engineered Energy Flows in Artificial Materials. *Phys. Rev. Lett.* **2002**, *89*, 186802.
(59) Bednarz, M.; Malyshev, V. A.; Knoester, J. Low-Temperature Dynamics of Weakly Localized Frenkel Excitons in Disordered Linear Chains. *J. Chem. Phys.* **2004**, *120*, 3827−3840.
(60) Akselrod, G. M.; Prins, F.; Poulikakos, L. V.; Lee, E. M. Y.; Weidman, M. C.; Mork, a. J.; Willard, A. P.; Bulović, V.; Tisdale, W. A. Subdiffusive Exciton Transport in Quantum Dot Solids. *Nano Lett.* **2014**, *14*, 3556−3562.
(61) Bardeen, C. J. The Structure and Dynamics of Molecular Excitons. *Annu. Rev. Phys. Chem.* **2014**, *65*, 127−148.
(62) Akselrod, G. M.; Deotare, P. B.; Thompson, N. J.; Lee, J.; Tisdale, W. A.; Baldo, M. A.; Menon, V. M.; Bulović, V. Visualization of Exciton Transport in Ordered and Disordered Molecular Solids. *Nat. Commun.* **2014**, *5*, 3646.
(63) Förster, T. Zwischenmolekulare Energiewanderung und Fluoreszenz. *Ann. Phys.* **1948**, *248*, 55−75.
(64) Wong, K. F.; Bagchi, B.; Rossky, P. J. Distance and Orientation Dependence of Excitation Transfer Rates in Conjugated Systems: Beyond the Förster Theory. *J. Phys. Chem. A* **2004**, *108*, 5752−5763.
(65) Baer, R.; Rabani, E. Theory of Resonance Energy Transfer Involving Nanocrystals: The Role of High Multipoles. *J. Chem. Phys.* **2008**, *128*, 184710.
(66) Cleary, L.; Cao, J. Optimal Thermal Bath for Robust Excitation Energy Transfer in Disordered Light-Harvesting Complex 2 of Purple Bacteria. *New J. Phys.* **2013**, *15*, 125030.
(67) For individual chromophores that have Gaussian homogeneous lineshapes, $k_{DA}(d_0, \varepsilon_D, \bar{\varepsilon})$ can be derived as[47,60]

$$k_{DA}(d_0, \varepsilon_D, \bar{\varepsilon}) = \frac{C}{\sqrt{2}}\left(\frac{2}{\varepsilon_D + \bar{\varepsilon} - \Delta_{ss}}\right)^4 \exp\left(-\frac{(\varepsilon_D - \bar{\varepsilon} - \Delta_{ss})^2}{4\sigma_h^2}\right),$$

where C is a constant as defined in eq 7. The maximum $k_{DA}(d_0,\varepsilon_D,\bar{\varepsilon})$ occurs at $\varepsilon_D = \Delta_{ss} + \sqrt{\bar{\varepsilon}^2 - 8\sigma_h^2}$. When $\sigma_h \ll \bar{\varepsilon}$, the result simplifies to yield the optimal donor energy to be $\varepsilon_D \approx \Delta_{ss} + \bar{\varepsilon}$.

(68) Talapin, D. V.; Koeppe, R.; Götzinger, S.; Kornowski, A.; Lupton, J. M.; Rogach, A. L.; Benson, O.; Feldmann, J.; Weller, H. Highly Emissive Colloidal CdSe/CdS Heterostructures of Mixed Dimensionality. *Nano Lett.* **2003**, *3*, 1677−1681.
(69) Meinardi, F.; Colombo, A.; Velizhanin, K. A.; Simonutti, R.; Lorenzon, M.; Beverina, L.; Viswanatha, R.; Klimov, V. I.; Brovelli, S. Large-area Luminescent Solar Concentrators Based on 'Stokes-Shift-Engineered' Nanocrystals in a Mass-Polymerized PMMA Matrix. *Nat. Photonics* **2014**, *8*, 392−399.
(70) Wang, F.; Beng Tan, W.; Zhang, Y.; Fan, X.; Wang, M. Luminescent Nanomaterials for Biological Labelling. *Nanotechnology* **2010**, *17*, R1−R13.
(71) Bässler, H. Charge Transport in Disordered Organic Photoconductors a Monte Carlo Simulation Study. *Phys. Status Solidi B* **1993**, *175*, 15−56.

DOI: 10.1021/acs.jpcb.5b01886
J. Phys. Chem. B XXXX, XXX, XXX−XXX

(72) As shown in ref 47, MSD grows nonlinearly initially in the presence of randomly oriented transition dipoles. However, this nonlinear feature appears to be small in the time-scale plotted in Figure 4 such that the MSD grows linearly with time.
(73) Fa, K.; Lenzi, E. Power Law Diffusion Coefficient and Anomalous Diffusion: Analysis of Solutions and First Passage Time. *Phys. Rev. E* **2003**, *67*, 061105.

DOI: 10.1021/acs.jpcb.5b01886
J. Phys. Chem. B XXXX, XXX, XXX−XXX